Contents lists available at ScienceDirect

Remote Sensing Applications: Society and Environment

journal homepage: http://ees.elsevier.com

Estimation of soil erosion risk in southern part of Syria by using RUSLE integrating geo informatics approach

Safwan Mohammed [a,*], Karam Alsafadi [b], Swapan Talukdar [c], Samer Kiwan [d], Sami Hennawi [d], Omran Alshihabi [e], Mohammed Sharaf [b], Endre Harsanyie [a]

[a] Institution of Land Utilization, Technology and Regional Planning, University of Debrecen, Debrecen, 4032, Hungary
[b] Department of Geography and GIS, Faculty of Arts, Alexandria University, Alexandria, 25435, Egypt
[c] Department of Geography, University of Gour Banga, Malda, 732101, India
[d] General Commission for Scientific Agricultural Research (GCSAR), Damascus, Syria
[e] Swedish University of Agricultural Sciences (SLU), Sweden

ARTICLE INFO

Keywords
Rill erosion
Agro-ecosystem
Erosivity
Erodibility
Mediterranean

ABSTRACT

Soil erosion is one of the major problems that threatens agricultural production and sustainability of natural resources in Syria. More than 85% of Syrian agricultural land is exposed to soil erosion at different rates. The present study estimated soil erosion in the eastern part of Yarmouk Basin in Al-Swida governorate (Southern Syria), by integrating the Revised Universal Soil Loss Equation (RUSLE) model and Geographic Information System (GIS) approach. The parameters used for the RUSLE model were prepared from climatic data, field data, and satellite imageries. Results showed that average erosivity was 374.19 MJ mm ha^{-1} h^{-1} yr^{-1}, while the K-factor ranged from 0.22 to 0.36 ton.ha.MJ^{-1}.mm^{-1}, and LS-factor reached 45% in some places. The estimated potential soil erosion ranged from 1.26 to 350.5 t ha^{-1} yr^{-1}, with an average of 137.4 t ha^{-1} yr^{-1}. Meanwhile, ninety-five percent of the study area experienced acceptable rate of erosion with soil loss, which ranged between 0 to 5 t ha^{-1} yr^{-1}. While, rest of the area experienced unacceptable erosion rate, which ranged from 5 to 350 t ha^{-1} yr^{-1}. Therefore, the areas which are experienced unacceptable erosion rate need immediate conservation plan from soil and water conservation point of view.

1. Introduction

Land degradation is one of the challenging issues in the 21st century. More than 6 billion hectares area affected by different types of land degradation around the world, such as soil sealing, soil erosion, soil contamination, salinization, soil compaction, acidification, and desertification (Wessels et al., 2007; Kertész, 2009; Inbar and Zgaier, 2016; Ganasri and Ramesh, 2016;). Meanwhile, to achieve the Sustainable Development Goals (UN-SDGs), healthy and high-quality soil is an essential requirement (Rodrigo-Comino et al., 2019).

Globally, soil water erosion is considered as a major cause of land degradation. Consequently, agricultural systems lost 75 billion tons of fertile soil annually (Sarapatka et al., 2018; Fu et al., 2005; Gomiero, 2016; Borrelli et al., 2017; Phinzi et al., 2020). From the environmental point of view, the effects of soil erosion cannot be estimated due to the complex interaction between the eroded soil and the different ecosystem components. The negative effects, include the soil fertility depletion, nutrient loss, and water pollution (Zhao et al., 2019; Tuo et al., 2018; Zhu, 2012; Pieri et al., 2014; Lal, 1998; Lu et al., 2004; Haregeweyn et al., 2015; Taye et al., 2018; Ekholm and Lehtorant, 2012).

Soil erosion monitoring is an essential tool for any kinds of land conservation plans. However, the experimental plots for measuring soil erosion are expensive and time consuming. Therefore, several models for estimating soil erosion have been developed and applied throughout the world. Researchers have been modelling the soil erosion for many decades. Approximately 82 soil erosion models, including the Universal Soil Loss Equation (USLE) (Wischmeier and Smith, 1965, 1978) and its revised version, named, RUSLE (Renard et al., 1991); Water Erosion Prediction Project (WEPP) (Nearing et al., 1989); and the European Soil Erosion Model (EUROSEM) (Morgan, 1995), have been using for soil erosion estimation (academics and decision-makers) (Karydas et al., 2014; Karydas and Panagos, 2018). Among them, the RUSLE model is considered as one of the widely applied empirical model for estimating soil water erosion.

García-Ruiz et al. (2013) reported that the soil in the Mediterranean basin is one of the world's soil erosion prone "hot spots". There are several reasons for the huge amount of soil loss in the Mediterranean basin, such as (1) rapid mineralization of organic matter

* Corresponding author.safwan@agr.unideb.hu

https://doi.org/10.1016/j.rsase.2020.100375
Received 31 December 2019; Received in revised form 23 July 2020; Accepted 5 August 2020
Available online xxx
2352-9385/

(OM) because of high temperature in summer and poor soil structure, (2) shallow soil with low erosion tolerance (T-factor), and (3) inadequate management of land-cover/vegetation cover due to overgrazing, and trampling, which badly affected ecosystem balance, plant growth, and soil recovery. Rare studies were carried out about the soil erosion in the eastern part of the Mediterranean basin, where Syria is located. Although a huge amount of soil loss has been observing in Syria for a long time. Nevertheless, several factors, such as intensive rainy storms, deforestation, burning of vegetation cover, and unsustainable agricultural practices, played an important role in accelerating soil water erosion (Kbibo et al., 2017; Mohammed et al. 2016, 2020a). In addition, the ongoing conflict has created a devastating impact on both the environmental and agricultural sectors (Abdo, 2018; Mohammed et al., 2019).

Unlike other Mediterranean countries, Syria has no strategies for soil conservation because of the lack of data for proposing plans and the absence of a clear vision for sustainable land resource management (Mohammed et al. 2020c). Therefore, the objective of this research was to delineate the soil erosion hazard area and estimate soil loss by using the RUSLE model. To the best of authors' knowledge, yet no studies have been carried out to integrate the geo-informatics and remote sensing approach for delineating and estimating the soil loss and erosion zones in the study area. Therefore, this study will provide important information for the development of soil erosion strategies that will be useful to policy makers, soil scientists and planners in effectively managing soil erosion in the study area.

2. Materials and methods

2.1. Area descriptions

The study area is located in the eastern part of the Yarmouk Basin in the Al-Swida governorate, in southern Syria (the geographical location is 32°28′15″N, 36°24′18″E and 32°46′44″N, 36°45′15″E) (Fig. 1). The climate is characterized by Mediterranean type (hot summer and rainy and moderately cool winter). The annual rainfall, ranges from 255 to 550 mm, happens mainly during the months of October to April. The average temperature is 21.5 °C. The main crops are grapes (*Vitissp*), apple (*Malus silvestris*), tomato (*Lycopersicum Esculentum*), water melon (*Citrullus Vulgoris*), and chickpeas (*Cicer Arictinum*). The study area is characterized by a steep plain in the eastern part, and more complex physiographical aspects in the western and northern parts. The elevation ranges from 696 m in the west to 1795 m in the east (Tall Qeni summit).

2.2. Soil samples and data collection

The target townships were identified based on the field survey, land use map, soil classification map, and climate variability. In this way, 56 representative soil profiles were prepared and described. 117 soil sam-

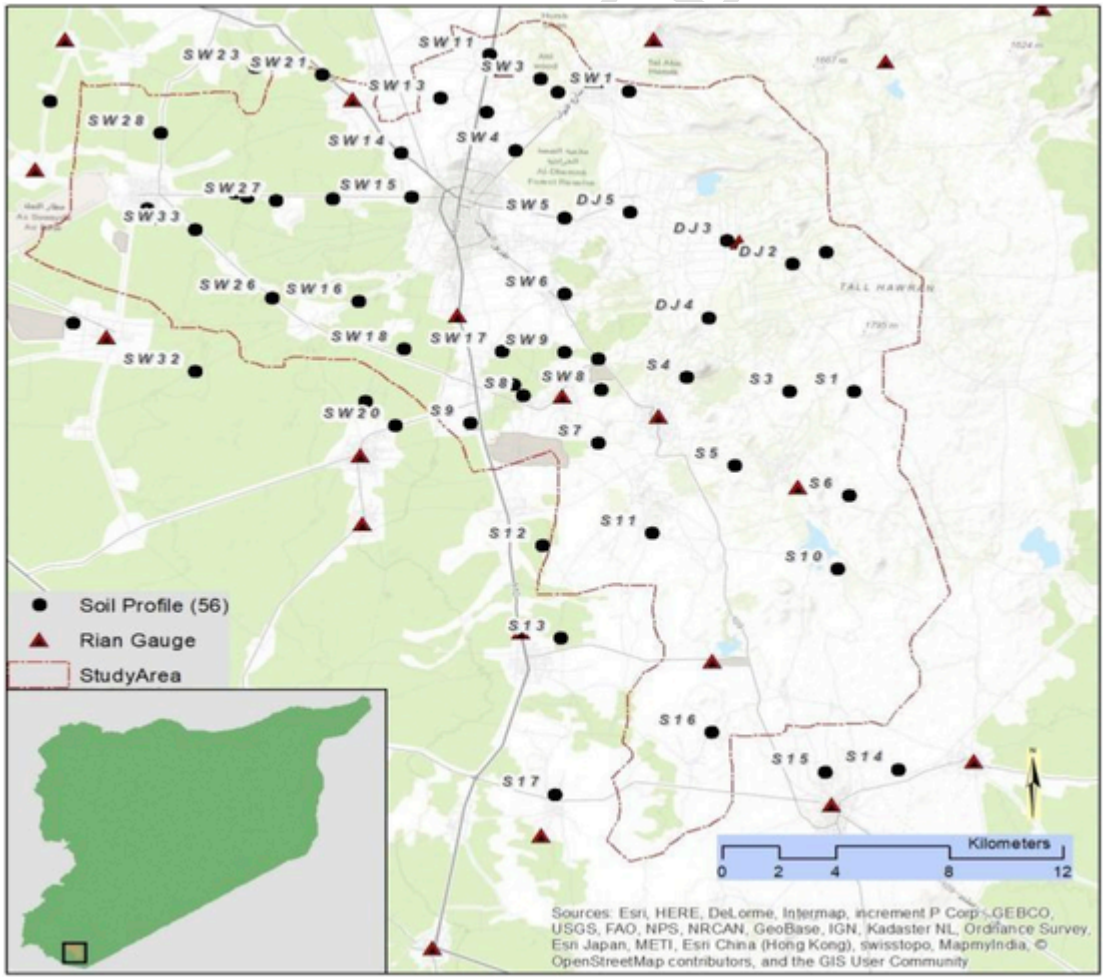

Fig. 1. Location of rain gauges and soil samples used in this study across the Western Slopes of Jabal Al-Arab in Southern Syria. The red triangles show the rain gauges used to estimate annual rainfall erosivity. The black circles are the soil samples locations. (For interpretation of the references to colour in this figure legend, the reader is referred to the Web version of this article.)

ples were collected (i.e. a sample from each horizon) from the field, and were brought to the soil laboratory in order to derive some essential physical and chemical components, such as soil texture (Day, 1965), and organic matter (%) (Nelson and Sommers, 1982) for calculating the K factor. Since soil water erosion affects only the topsoil layer (0–25 cm), thus, the top soil analysis data were only used for calculating K factor (i.e. 56 soil samples). More details about physico-chemical soil properties can be found in Mohammed et al. (2020b).

Monthly rainfall data of 16 climatic stations were obtained from Ministry of Agriculture (MoA), General Commission for Scientific Agricultural Research (GCSAR), and Syrian Meteorological Authority (SMA) for the period of 1975–2010. The DEM (Digital Elevation Model; 12.5 × 12.5m resolution) was obtained from the Advanced Land Observing Satellite (ALOS) (https://www.asf.alaska.edu/sar-data/palsar/). It was used to generate slope and elevation of the study area. GIS analysis was conducted in the ArcGIS 10.5 software environment. The list of the data sources was summarized in Table 1. The methodological steps can be seen in Figure (2).

Table 1
Details of the data used in the present study.

No.	Data type	Format	Factor	Source	Description
1	Soil data	Excel (*.xls)	K	Field Survey	56 soil profiles, 56 samples, soil texture and OM (%)
2	Rainfall data	Excel (*.xls)	R	Ministry of Agriculture and GCSAR; Syria, Syrian Meteorological Authority	Monthly rainfall data for 17 stations from 1975 to 2010
3	Satellite Image	Raster (.tif)	C	Bing Map Image	Spatial Resolution 8 *8m
4	DEM	Raster (.tif)	LS, P	ASF: The Alaska Satellite Facility, ALOS	Spatial Resolution 12.5*12.5 m

2.3. Estimation of the input parameters used for RUSLE model

The well-known RUSLE model (Renard et al., 1991) has been extensively applied for estimating sheet and rill erosion rates (Zerihun et al., 2018) based on five parameters (rainfall, soil, topography and slope, land cover, and support practice) using equation (1):

$$A = \mathbf{R}.\mathbf{K}.\mathbf{LS}.\mathbf{C}.\mathbf{P} \quad (1)$$

where A denotes the Soil Loss ($t.ha^{-1}.yr^{-1}$), R refers to the Rainfall Erosivity ($MJ.mm.\ ha^{-1}.\ h^{-1}.\ Yr^{-1}$), K represents the Soil Erodibility ($ton.ha.MJ^{-1}.mm^{-1}$), LS denotes the Topographic factor, C refers to the Cover Management, and P denotes the Support Practice.

2.3.1. Rainfall erosivity (R)

The intensity and duration of rainstorms affect the stability of soil aggregates, especially when it exceeds the soil resistance which causes more soil water erosion (Ollobarren Del Barrio et al., 2018). R factor represents the kinetic energy of raindrops, which causes erosion (Nampak et al., 2018). Wischmeier and Smith (1978) proposed a formula to calculate R factors by multiplying the kinetic energy of a rainstorm and its maximum 30 min intensity (I_{30}). However, due to the lack of I_{30} data within the study area, we followed equation (2) as

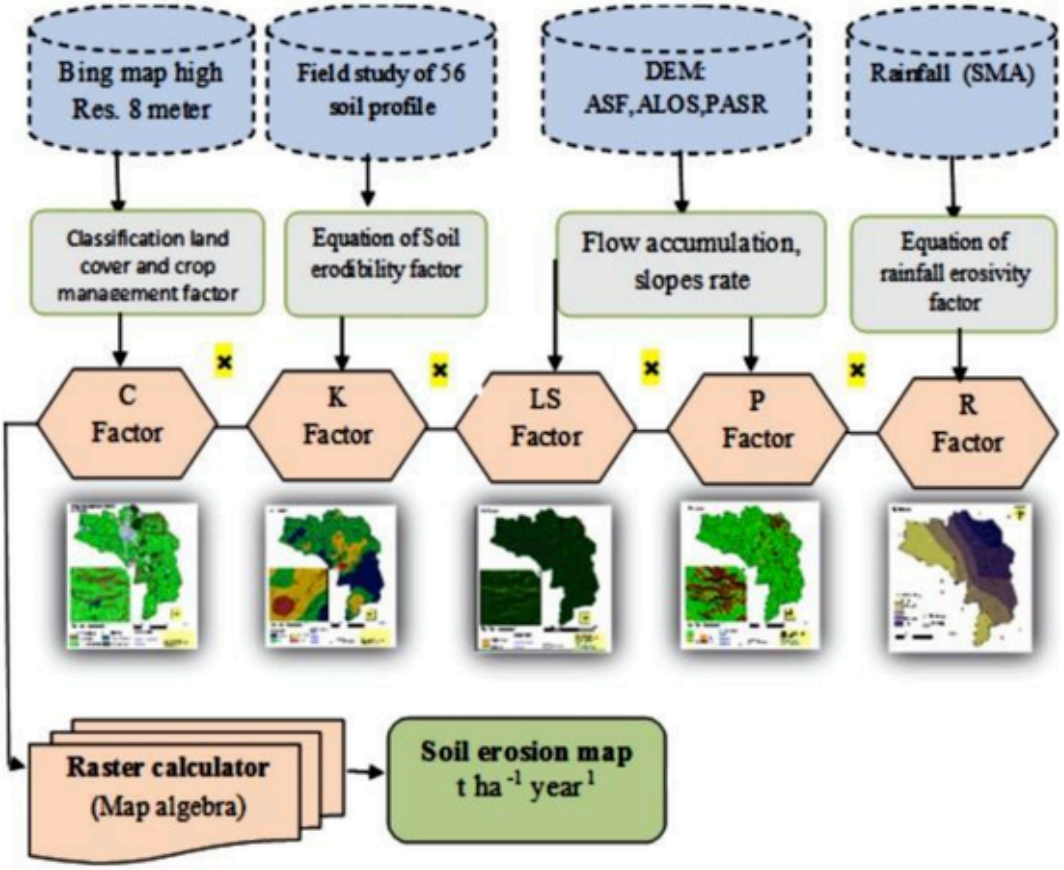

Fig. 2. Flow chart of the methodology.

a proxy of I_{30} for calculating the R factor (Arnoldus, 1980; Sujatha and Sridhar, 2018; Prasannakumar et al., 2011b).

$$R = \sum_{i=1}^{12} 1.75 * 10^{\left(1.5\log_{10}\left(\frac{p_i^2}{P}\right) - 0.8188\right)} \quad (2)$$

where R is the rainfall erosivity factor (MJ mm ha^{-1} h^{-1} per year), p_i is the monthly rainfall (mm), and P is annual rainfall (mm).

Monthly precipitation data from 16 stations of the study area were used to calculate the R factor (Table 2). Ultimately, the data was imported to ArcGIS software and interpolated using the 'Kriging' method. Notably, the Kriging method was adopted in this research because it has the best fitting according to our data and less error (unpublished data).

2.3.2. Soil Erodibility (K)

The *K* factor reflects the soil resistance to both the detachment and transportation (Renard et al., 1997; Chang et al., 2015). Generally, *K* factor, ranges from 0 to 1, is considered as a reflection of soil characteristics, such as texture, organic matter (%), and unsaturated hydraulic conductivity. Based on the findings from the laboratorial analysis, the K factor was calculated by following Sharply and Williams' (1990) method (equation (3)).

$$K = 0.2 + 0.3e^{0.02*SAN\left(1-\frac{SIL}{100}\right)} * \left(\frac{SIL}{CLA}\right)^{0.3} * \left(1 - \frac{0.25OM}{OM + e^{(3.72-2.95OM)}}\right) * \left(1 - \frac{0.7 * SN_1}{SN_1 + e^{(22.9SN_1 - 5.51)}}\right) \quad (3)$$

where SAN = sand (%), SIL = silt (%), CLA = clay (%), OM = organic matter (%), $SN_1 = \frac{1-SAN}{100}$.

Then, the K factor was mapped by kriging interpolation in ArcGIS software.

2.3.3. Topographic factor (LS)

The geomorphology of the study area contributes significantly to soil erosion through slope length (L) and slope steepness (S) (Da Cunha et al., 2017; Ozsoy et al., 2012). In the present study, LS factor was calculated from DEM (spatial resolution: 12.5 m) by following the method of Moore and Burch (1986) (equation (4)) in ArcGIS 10.5 software (Benchettouh et al., 2017; Dutta et al., 2015).

$$LS = \left(flow\ accumulation * \frac{Cell\ size}{22.1}\right)^{0.4} * (sin\ slope * 0.896)^{1.3} \quad (4)$$

The slope percentage of the study area was prepared from the DEM, then the topographic factor (LS map) was generated.

2.3.4. Cover Management Factor (C)

In soil erosion studies, C Factor is highly correlated to the land use/land cover practice, because of its dependence on crop rotation, agricultural practice, vegetation canopy, surface roughness, and sub-surface biomass (Chen et al., 2019; Sujatha and Sridhar, 2018). The C Factor ranges between 1 and 0, while closeness to 0 indicates the well protected land (Ganasri and Ramesh, 2016). Since, there was an absence of measurement/data for the C-Factor in Syria, it was generated from Bing satellite image. The supervised classification method was applied for classifying the land use land cover map, then it was multiplied by the values proposed by Ganasri and Ramesh (2016) to calculate C factor (Table 3).

2.3.5. Support practice factor (P)

Support Practice Factor (P) is one of the important factors that plays a vital role in controlling the soil erosion by minimizing its potential hazard. P values range from 0 to 1, while closeness to 1 indicates the absence of conservation practice and vice versa (Mahala, 2018; Das et al., 2018). In the present study area, we observed some support practices like traditional agriculture, such as terraces (it is traditionally used to hedge soil). While, other studies in Syria assumed 1 as P factor (Abdo, 2018; Abdo and Salloum, 2017). The P factor for this research was calculated by following Morgan (2005), Panagos et al. (2015) and Toubal et al. (2018) (Table 4).

2.4. Estimation of annual soil loss rate

The RUSLE model was applied on the aforementioned parameters (pixel-by-pixel) to generate soil erosion map in the study area. The whole work was done in ArcGIS software.

Table 2
Calculation of R factor for 16 stations of the study area.

ID	Data Source	Y	X	R
1	GCSAR	32.698797	36.671557	603.4976
2	GCSAR	32.669815	36.566274	302.4508
3	GCSAR	32.85528	36.628566	329.9084
4	GCSAR	32.493165	36.711794	298.4524
5	GCSAR	32.60947	36.695964	452.6098
6	GCSAR	32.634455	36.642838	518.9619
7	GCSAR	32.510163	36.764892	436.6879
8	GCSAR	32.554227	36.593472	267.4414
9	SMA	32.766078	36.724414	613.4459
10	SMA	32.79484	36.505539	239.6074
11	SMA	32.592638	36.533109	203.5635
12	SMA	32.719735	36.406236	171.8381
1	SMA	32.545033	36.665797	298.8923
13	SMA	32.510283	36.7632	434.3739
14	SMA	32.617782	36.531569	214.6772
15	SMA	32.772295	36.637396	730.9282
16	SMA	32.827376	36.706246	243.8814

Table 3
Land use/land cover classes and respective C-factor value.

No	Land Use	Area (km2)	%	C Factor
1	Forest	28.4	5.50	0.003
2	Agricultural	350.06	67.83	0.63
3	Waste Land	34.98	6.77	0.5
4	Built Up	100.4	19.46	0.09
5	Water Body	2.14	0.41	0

Table 4
P value for different slope gradient.

Slope (%)	P-factor
9–12	0.6
13–16	0.7
17–20	0.8
21–25	0.9
>25	0.95

3. Results

3.1. Rainfall erosivity (R)

Average rainfall in the study area ranged between 216.74 mm and 541.51 mm, which produced an average erosivity of 374.19 MJ mm ha^{-1} h^{-1} yr^{-1}. The spatial distribution of R factor showed a clear zone between the northern part (having high R value) and the southern part (having low R value). It highlighted the role of topography, as the mountains are found in the northern part (Fig. 3).

3.2. Soil Erodibility (K)

More than 80% of soil samples were clayey texture. While, the OM (%) ranged between 0.6 and 6.3%. Therefore, the K-factor ranged from 0.22 to 0.36 ton.ha.MJ^{-1}.mm^{-1} (Fig. 4). The K values ranged between 0.25 and 0.3 ton.ha.MJ^{-1}.mm^{-1} in the major parts of the study area.

3.3. Topographic factor (LS)

The slope percentage ranged between 4 and 45% in the study area, while the LS-factor reached to 45% in some places (Figs. 5 and 6). High LS-factor was observed in the steep slopes in the northern part of the study area, such as the high hills and the mountains (Thomas et al., 2018).

3.4. Cover Management Factor (C)

The study area was categorized into five land use land cover classes by using supervised image classification. The final map (Fig. 7) showed that the majority of the study area has agricultural area, while the rest of the study area has been dominated by forests, followed by waste land, built-up land, and water bodies. Based on the land use land cover types in the study area, high C-values were observed in agricul-

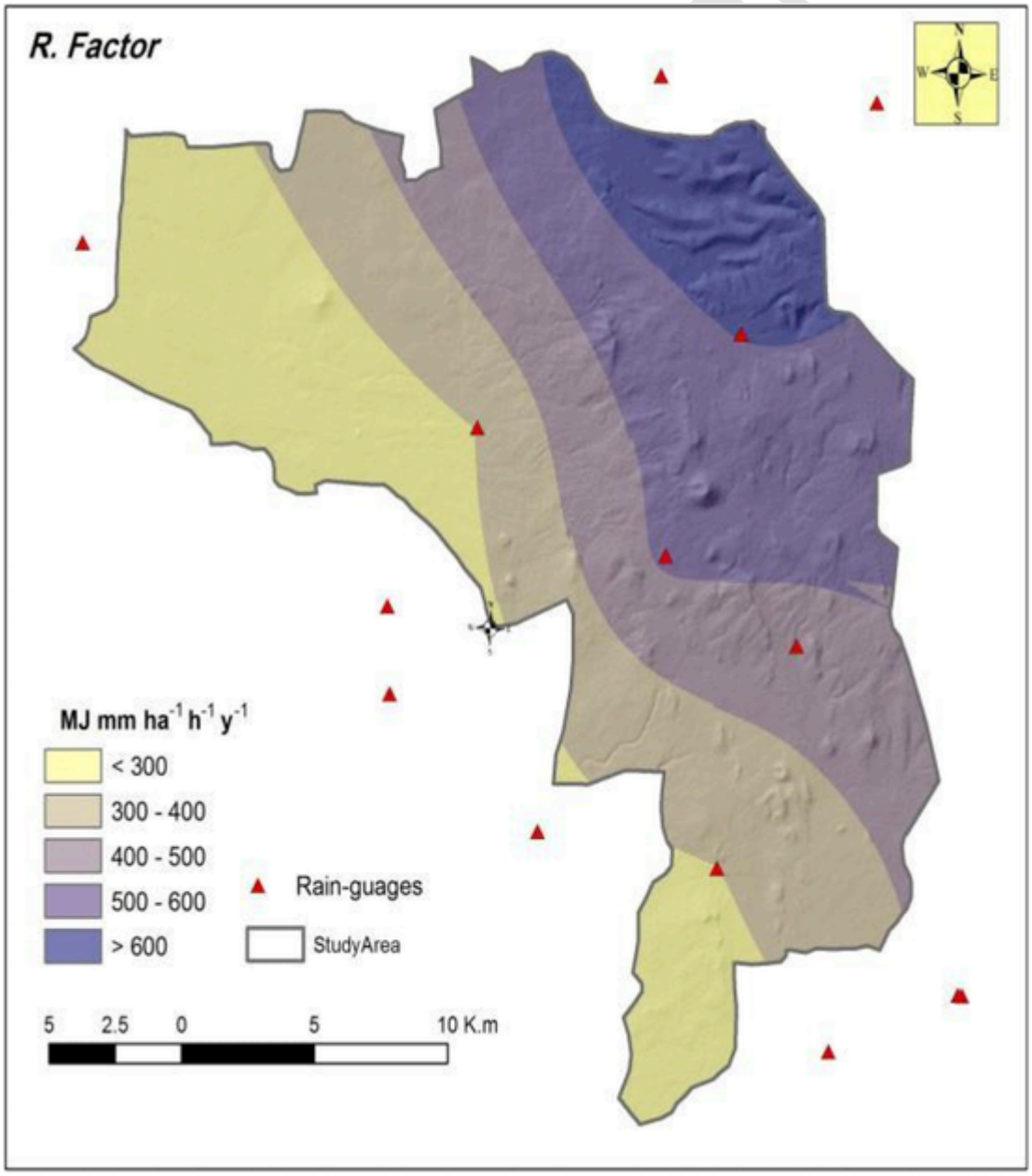

Fig. 3. Rainfall erosivity factor (R).

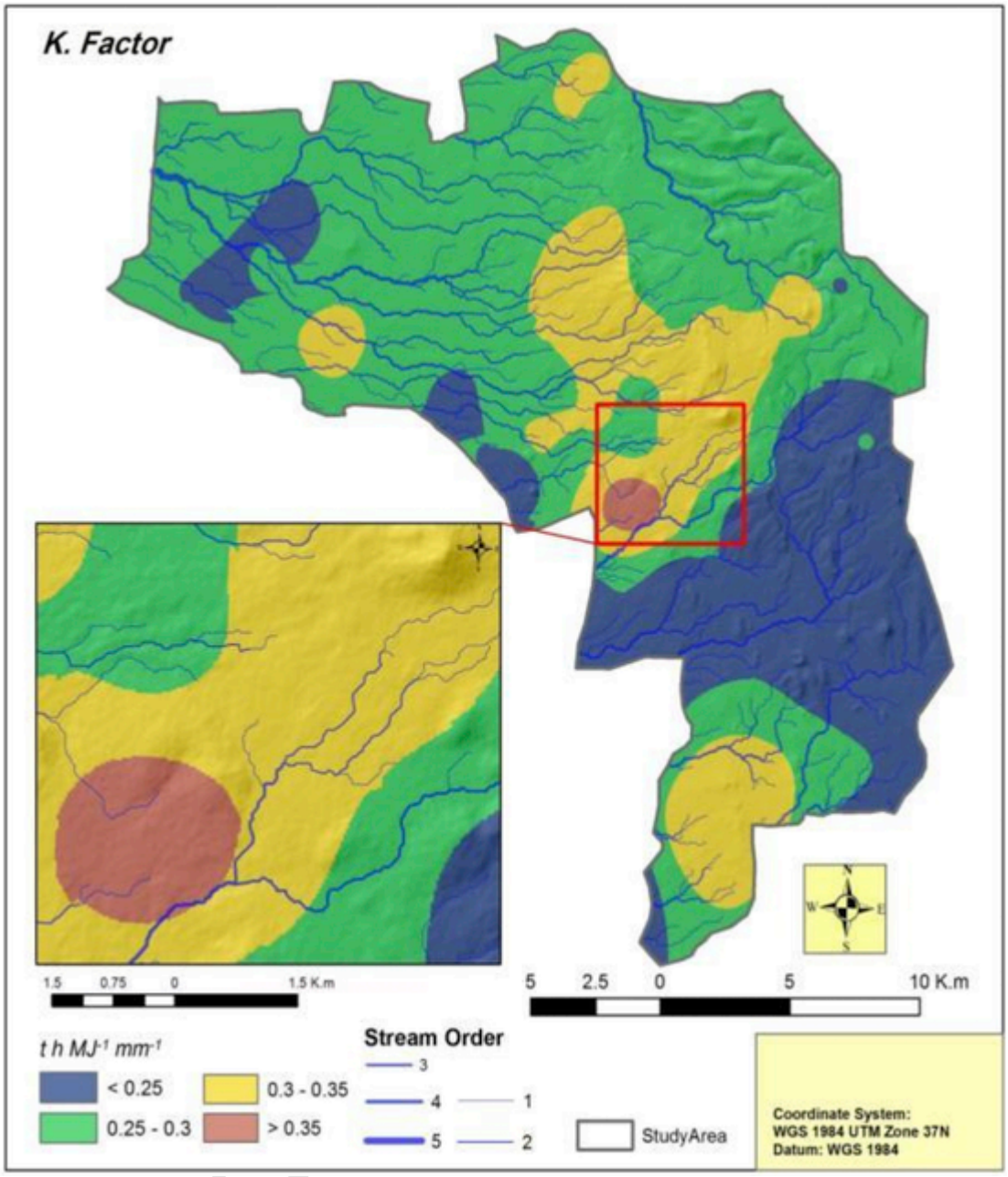

Fig. 4. Soil Erodibility factor (K).

tural areas and waste land indicating higher potentiality for soil erosion in those areas due to different land use practices, such as tillage (Woldemariam et al., 2018; Biswas and Pani, 2015).

3.5. Support practice factor (P)

Approximately 90% of the study area had P factor of 0.6–0.7 (Fig. 8). The highest value (0.7–0.95) was observed in the northern part of the study area, where high hills are located.

3.6. Estimation and spatial distribution of annual soil erosion

The soil erosion map was generated by using the RUSLE model. Results showed that the annual soil erosion ranged from 1.26 to 350.5 t ha^{-1} yr^{-1}, with the average of 137.4 t ha^{-1} yr^{-1} (Fig. 9). Interestingly, the areas, had high risk of soil erosion, were located in the northern mountainous part of the study area. This finding was quite expected, because the area was characterized by high rain intensity and sharp slopes, and absence of soil conservation practices.

The soil erosion zone in the study area was classified into 5 classes, such as acceptable, moderate, high, severe and extreme (Table 5). Results showed that about 95% of the area was classified as the acceptable erosion zone (Table 5)

Table 6 revealed that agricultural land was the most soil erosion affected area by, followed by the waste land. Remarkably, 20 km^2 of agricultural land experienced erosion more than 5 t h^{-1} yr^{-1}, which was quite high in the study area. The lowest amount of soil erosion was found in the forest area, where the canopy cover acted as the blanket cover to prevent the destructive impact of rain drops.

Table 7 explicated the statistical analysis of soil erosion for each land cover. The results showed that 67.83% of the study area was covered by agricultural land, where the average erosion

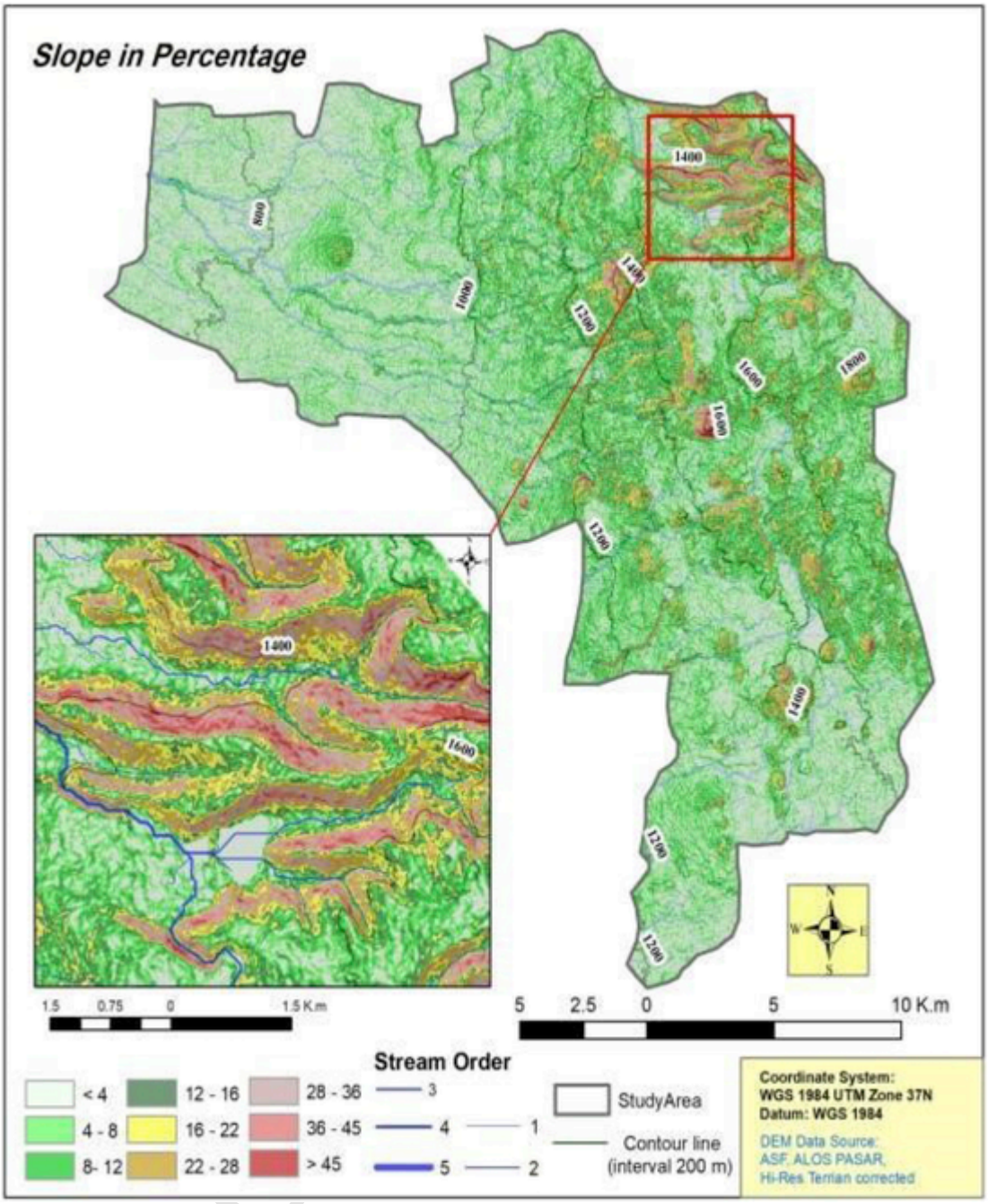

Fig. 5. Slope map in percentage.

reached 1.22 t h^{-1} yr^{-1}.The maximum erosion in agricultural land was exceeded 250 t h^{-1} yr^{-1}. Surprisingly, the maximum erosion was recorded in waste lands (350 t h^{-1} yr^{-1}), which covered only 6.77% of the study area. Thus, it could be considered as less of a priority.

4. Discussion

Soil erosion is a major threat to sustainability of land resources in Syria. Studies show that the eastern and northern part of the study area are subjected to wind erosion (Masri et al., 2003), while the western and the southern part are more prone to the soil water erosion (Mohammed et al., 2016). In the present study, multiple data, such as satellite imageries, soil data, and rainfall data were integrated to generate the potential soil erosion hazard map. Result revealed that the majority of the study experienced erosion rate of 1–5 t $ha^{-1}.y^{-1}$. Similar findings have by Djoukbala et al. (2018) who reported estimated 3 to 5.7 t $ha^{-1}.y^{-1}$ of annual soil loss in Wadi El-Ham watershed, whereas Paroissien et al. (2015) estimated an average soil loss of 4.2 t $ha^{-1}.y^{-1}$ in Languedoc water shade in Peyne, France. Also, Fang et al. (2019) reported that the Yangtze river basin of China experienced average soil loss of 3.89 t $ha^{-1}.y^{-1}$. Thomas et al. (2018) predicted the average soil erosion of 3.60 t $ha^{-1}.y^{-1}$ in Muthirapuzha river basin (Western Ghat, India).

Similar to Abdo and Salloum (2017), our results indicate that only 5% of the study area observed high soil erosion. Abdo and Salloum (2017) reported that 4% of the area in the Alqerdaha basin of Syria observed high soil erosion rate. In addition, Demirci and Karaburun (2012) found 5% of Buyukcekmece watershed lake, North-

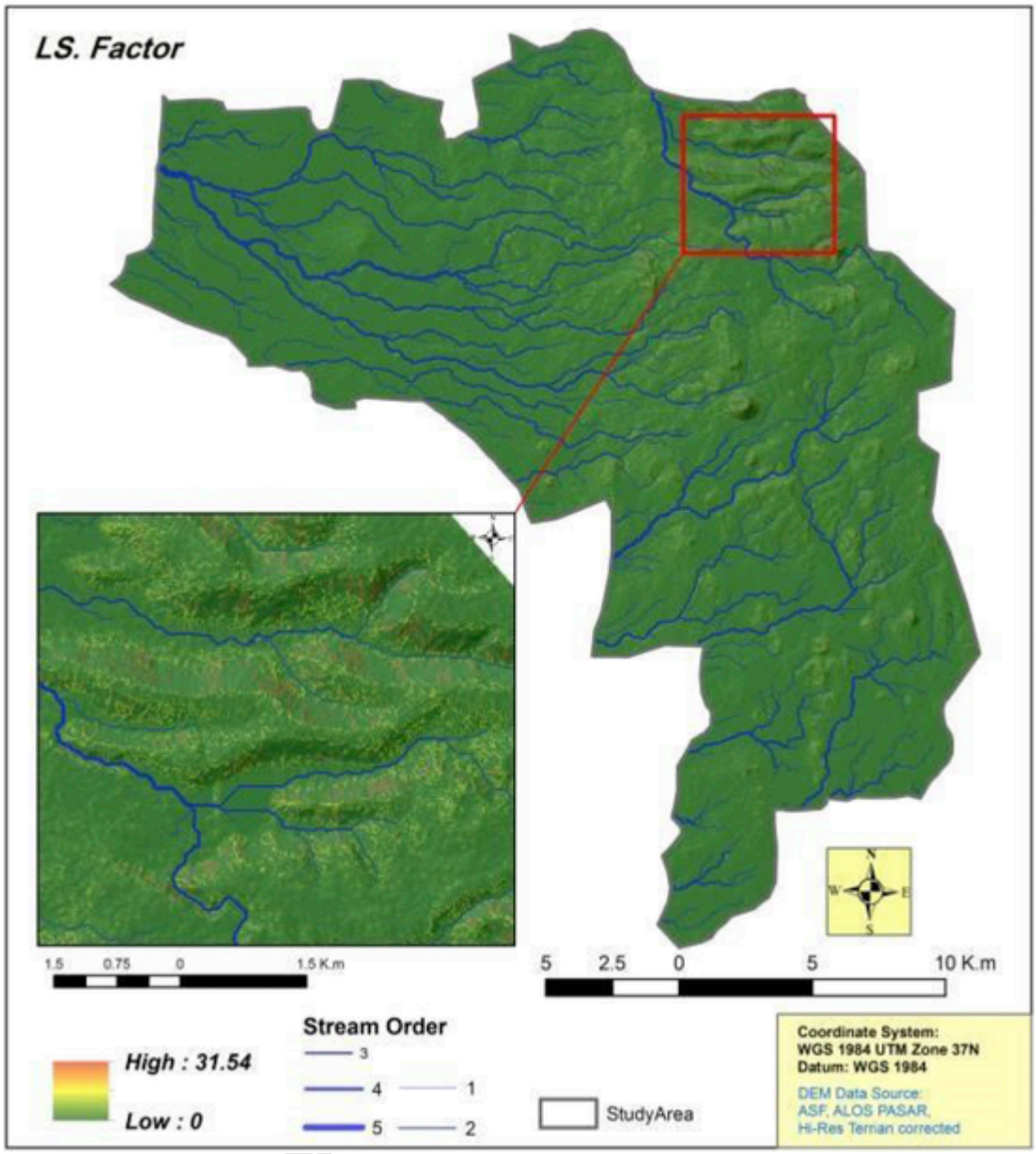

Fig. 6. Topographic factor (LS).

west Turkey has high or severe soil erosion rate. Markose and Jayappa (2016) however predicted a higher rate of erosion in Kali river basin (Karnataka, India). The high soil erosion prone areas found in the mountain slopes and steep terrain highlights the importance of topographic factor in influencing soil water erosion in the southern part of Syria and elsewhere. Thomas et al. (2018) reported that severe soil erosion was observed in the steep slope of the mountainous region of Muthirapuzha river basin of India. Zerihun et al. (2018) estimated the severe soil loss in the steep slope areas of NW Ethiopia. Kayet et al. (2018) found that the steep slope regions of the West Singbhum district of Jharkhand (India) were highly suffered by the high soil erosion rates. According to Prasannakumar et al. (2012), the predicted maximum soil loss (17.73 t $ha^{-1}.y^{-1}$) occurred in the high slope areas of the small mountainous river basin of Kerala, India. Our findings (Table 7) indicates that agricultural land and waste land appears to promote soil erosion in the study area. Similar result can be found in the work of Fayas et al. (2019), Das et al. (2018), Da Cunha et al. (2017), Hao et al. (2017), Gandino et al. (2016), Ganasri and Ramesh (2016), Morgan (1995). Therefore, based on the findings of previous literature, the findings of the current work can be considered as valid. Hence, it can be adopted for identifying the soil erosion zones and used for proposing the soil conservation plans in the identified high soil erosion areas.

The R factor in the study area ranged between 171.8-730.9 MJ mm ha^{-1} h^{-1} per year, while, Hasan et al. (2014) reported that the average R value was 491 MJ mm ha^{-1} h^{-1} yr^{-1} in the Zgaro River of Western Syria. Ferreira and Panagopoulos (2014) estimated the average R value between 80.4-854 MJ mm ha^{-1} h^{-1} per year in the Mediterranean conditions in Alqueva dam watershed, Portugal. Farhan and Nawaiseh (2015) predicted the average R values between 54.3-227.12 MJ mm ha^{-1} h^{-1} in the Wadi Kerak catchment of Lisan Peninsula. Farhan et al. (2013) reported the average rainfall erosivity ranges between 85.4-420.6 MJ mm ha^{-1} h^{-1} per year in the Kufranja watershed, Northern Jordan. Ozsoy et al. (2012) estimated the average value of the R factor ranges between 513-2658 MJ mm ha^{-1} h^{-1} per year in Mustafa Kemal river basin, Turkey. They also reported

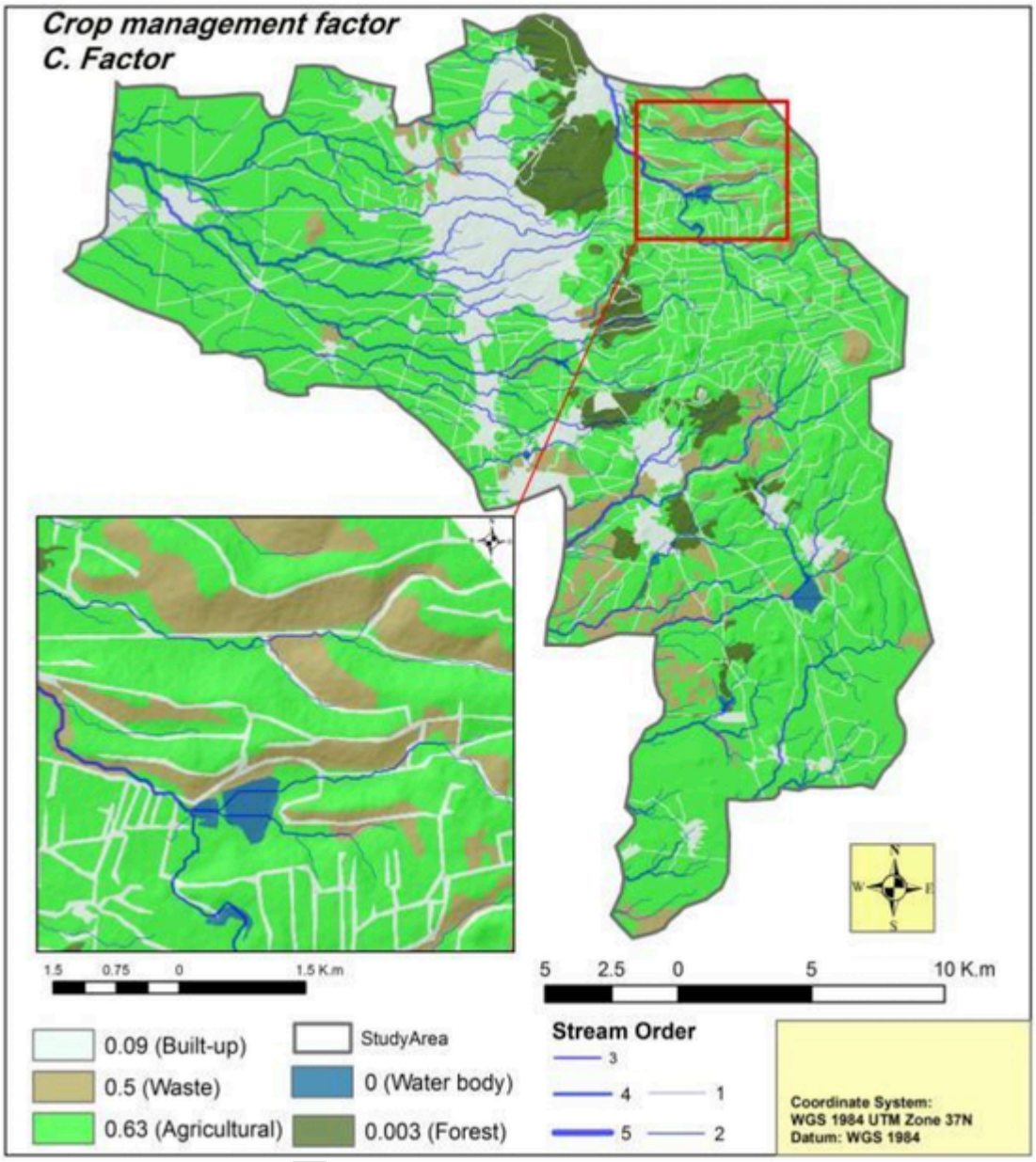

Fig. 7. Cover management factor (C).

that the erosivity factor is mostly dependent on the rainfall, therefore, it could not be considered the base value of the neighbour areas. Pal (2016) recommended that the erosivity factor must be calculated from the rainfall of investigated areas and could be compared with the areas having very similar climatic characteristics. The value of the R factor in the present study area was quite identical with the mentioned studies, which were conducted in Mediterranean regions. Therefore, the calculated R factor can be considered as the base for further research and policy making in the study area.

The K value varied from <0.25 to >0.35 ton.ha.MJ^{-1}.mm^{-1}, where low K value was recorded in the clayey soil. Das et al. (2018) reported the K value ranges between 0.16-0.28 ton.ha.MJ^{-1}.mm^{-1} in Tirap district, Arunachal Pradesh (India). Farhan and Nawaiseh (2015) calculated the K value ranges between 0.1-0.4 ton.ha.MJ^{-1}.mm^{-1} in Wadi Kerak catchment of Lisan Peninsula. Kayet et al. (2018) estimated the K value between 0.12-0.42 ton.ha.MJ^{-1}.mm^{-1} in West Singhbhum district of Jharkhand, India. They reported that the low K value was found in the clay soils because these were exposed to handicap. While the high K value could be observed in the silt loam soils, because (1) the soil particles are abstemious to purely detachable, (2) infiltration is sensible to small generating the modest to high runoff, and (3) the sedimentation is moderate to move simply. Similarly, Fu et al. (2011), Nasir and Selvakumar (2018) also explained the causes of the lower K value in the clay texture and reported that it is less detachable with the high resistance to the rain drop forces. A high content of organic matter with very fine texture (clay) and good hydraulic conductivity (good infiltration ratio) reduce the potentiality of the soil erosion (Kayet et al., 2018; Pal and Debanshi, 2018). To the contrary, it leads to a high probability of the soil being exposed to water erosion. Thus, low K value in the study area represented the low soil detachability and less vulnerability to soil erosion.

The northern part of the study area had the higher LS-factor ($>40\%$). Generally, the soil erosion is not a major problem in flatlands, but it is worse in the high elevated areas or steepness areas. The high LS-factor may be because of the high rainfall intensity in this area

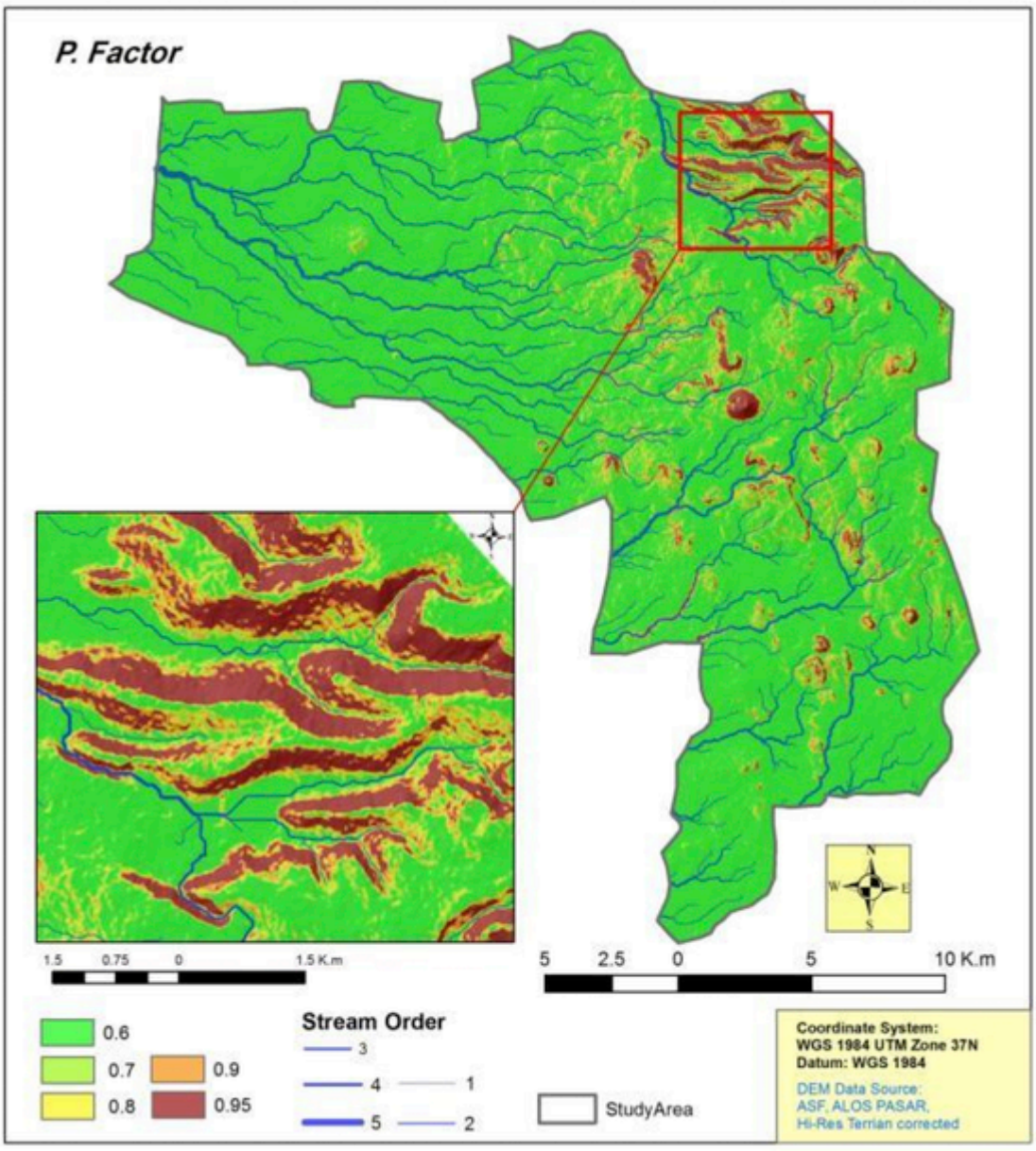

Fig. 8. Conservation support practice factor (P).

and the deteriorated vegetation cover, which cause higher cumulative runoff (Prasannakumar et al., 2011a; Ostovari et al., 2017). Abdo (2018) noted that the hilly terrain with steep slopes accelerated the soil erosion in the coastal region of Syria (western part). Similarly, Kbibo et al. (2017) reported that high slope leading to the increase in soil erosion, as a function of the topography, regardless the type of vegetation cover in the coastal mountains of Syria. Thus, the higher rate of soil erosion is expected in the northern part of the study area.

Land cover reflects the impact of soil cover on the total erosion. The majority of the study area dominated by the agricultural land and consequently, the C factor was high (0.63). While minimum value was observed in the forest area (0.003). The main crop production is viticulture in the study area, which occupies about 10125 ha (Alsafadi et al., 2019). Studies show that the cultivation of vineyard in Mediterranean region exacerbate soil erosion because the soil remains bare and exposed to the intensive rain storms, which enhanced the soil sealing and accelerates runoff generation (Martínez-Casasnovas and Sánchez-Bosch, 2000; Cerdà et al., 2020; Remke et al., 2018; Rodrigo-Comino et al. 2018b). Farmers in the study area, as well as in the sem-iarid regions, have the tendency to keep the soil bare in vineyard fields to prevent the competition for water and nutrients (Raclot et al., 2009; Rodrigo-Comino, 2018a). All of these factors make the agricultural lands more susceptible to erosion.

Even though some uncertainties could occur, the land conservation plans in the study area can rely on the RUSLE model. Results would be very useful and valuable to the decision makers for delineating the most susceptible region to the soil erosion hazard. Therefore, this study would help in shaping not only regional conservation plans, but could be extended in national level for proposing the soil conservation plans.

5. Conclusion

In light of the paucity of sufficient information about soil erosion in Syria, this study attempted to outline the situation of the soil water erosion in the southern region of Syria. The integration of GIS and remote sensing technology played a key role to estimate the soil erosion risk in a simple, easy and scientific way. Potential soil erosion ranged

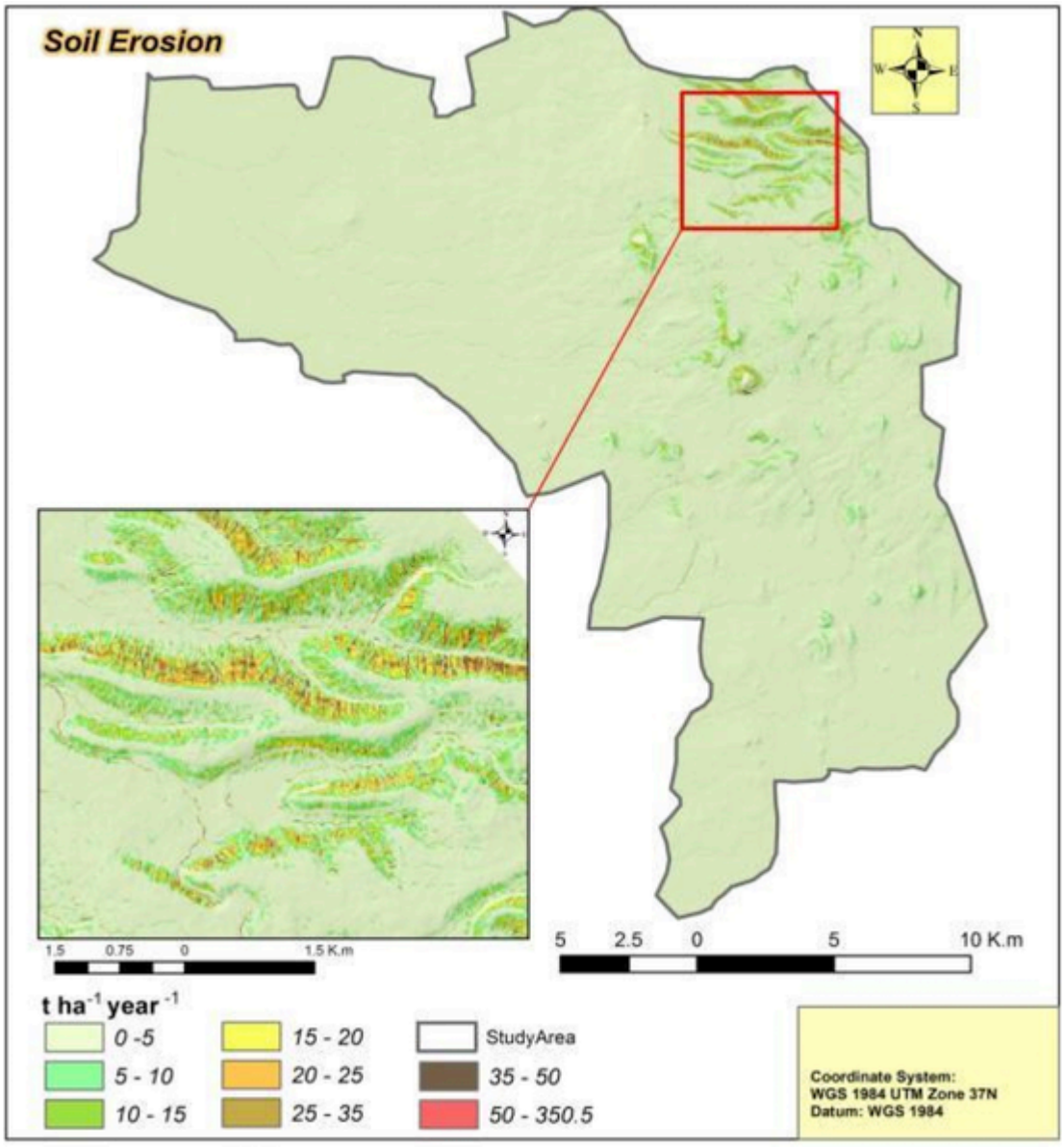

Fig. 9. Spatial distribution of annual soil loss (t $h^{-1}y^{-1}$).

Table 5
Soil loss distribution in the study area.

Erosion classes	Soil loss (t h^{-1} y^{-1})	Area (km ^{2})	Percentage
Acceptable	0–5	490.48	94.74
Moderate	5–10	13.65	2.65
High	10–15	5.54	1.07
Severe	15–20	2.788	0.54
Extreme	>20	3.53	1

Table 6
Distribution of the areas (km ^{2}) in different erosion levels in each land cover type.

Soil loss (t h^{-1} yr^{-1})	Forest	Water body	Waste Land	Agricultural land	Built-Up
0–5	28.40	0	29.48	332.2	100.2
5–10	0	0	2.72	10.80	0.12
10–15	0	0	1.35	4.15	0.01
15–20	0	0	0.66	2.1	0.004
>20	0	0	0.72	2.8	0.002

from 1.26 to 350.5 t ha^{-1} yr^{-1}. Where, 5% of the study area observed the extreme erosion risk. Based on the findings, this study recommends the implementation of an immediate soil conservation practice such as agri-spillways; conservation tillage; buffer strips and minimum cultivation; and soil terracing in the most threatened areas, especially in the northern part of the study area. For further studies, experimental plots should be conducted to validate the RUSLE model. Meanwhile, decision makers should carry out a future development plan in a more scientific way for soil conservation in the study area.

Author statement

Safwan Mohammed: Conceptualization, Methodology, Writing - original draft. Karam Alsafadi: Methodology, Visualization, Swapan Talukdar: Writing - review & editing, Supervision, Samer Kiwan

Table 7
Zonal Statistical analysis of soil erosion for each land cover types.

Land cover	Soil loss (t h $^{-1}$ yr $^{-1}$)				
Land cover	Area/km ^{2}	%	Max	Mean	Standard deviation
Forest	28.40	5.50	1.26	0.009	0.02
Water Body	2.14	0.41	0	0	0
Waste Land	34.97	6.77	350.56	2.62	6.05
Agricultural land	350.06	67.83	277.19	1.22	3.63
Built-Up	100.43	19.46	58.19	0.171	0.49

and Sami Hennawi fled survey and data collection; Omran Alshiehabi: Writing - review & editing. Mohammed Sharaf and Endre Harsanyie: Supervision.

Declaration of competing interest

The authors declare that they have no known competing financial interests or personal relationships that could have appeared to influence the work reported in this paper.

Acknowledgment

The authors grateful for Damascus and Debrecen Universities for their unlimited support. Authors also thank the staff members at General Commission for Scientific Agricultural Research (GCSAR), Damascus, Syria; Faculty of Agricultural, Department of Soil Science, Damascus University, Damascus, Syria for their help with sample analysis. Also authors grateful for the editors and anonymous reviewers for constructive comments and suggestions to considerably improving the quality of this manuscript.

Appendix A. Supplementary data

Supplementary data to this article can be found online at https://doi.org/10.1016/j.rsase.2020.100375.

Uncited references

Abdo, 2017; National Weather Service, 2000; Pimentel and Burgess, 2013.

References

Abdo, H, 2017. Geo-Modeling approach to predicting of erosion risks utilizing RS and GIS data: a case study of Al-Hussain Basin, Tartous, Syria. J Environ Geol. 1 (1), 1–4.
Abdo, H G, 2018. Impacts of war in Syria on vegetation dynamics and erosion risks in Safita area, Tartous, Syria. Reg. Environ. Change 1–13.
Abdo, H, Salloum, J, 2017. Spatial assessment of soil erosion in Alqerdaha basin (Syria). Modeling Earth Systems and Environment 3 (1), 26.
Alsafadi, K, Mohammed, S, Habib, H, Kiwan, S, Hennawi, S, Sharaf, M, 2019. An integration of bioclimatic, soil, and topographic indicators for viticulture suitability using multi-criteria evaluation: a case study in the Western slopes of Jabal Al Arab—Syria. Geocarto Int. 1–23.
Benchettouh, A, Kouri, L, Jebari, S, 2017. Spatial estimation of soil erosion risk using RUSLE/GIS techniques and practices conservation suggested for reducing soil erosion in Wadi Mina watershed (northwest, Algeria). Arabian Journal of Geosciences 10 (4), 79.
Biswas, S S, Pani, P, 2015. Estimation of soil erosion using RUSLE and GIS techniques: a case study of Barakar River basin, Jharkhand, India. Modeling Earth Systems and Environment 1 (4), 42.
Borrelli, P, Robinson, D A, Fleischer, L R, Lugato, E, Ballabio, C, Alewell, C, Bagarello, V, 2017. An assessment of the global impact of 21st century land use change on soil erosion. Nat. Commun. 8 (1), 2013.
Cerdà, A, Rodrigo-Comino, J, 2020. Is the hillslope position relevant for runoff and soil loss activation under high rainfall conditions in vineyards? Ecohydrol. Hydrobiol. 20 (1), 59–72.
Chang, T J, Zhou, H, Guan, Y, 2015. Applications of erosion hotspots for watershed investigation in the Appalachian Hills of the United States. J. Irrigat. Drain. Eng. 142 (3), 04015057.
Chen, Z, Wang, L, Wei, A, Gao, J, Lu, Y, Zhou, J, 2019. Land-use change from arable lands to orchards reduced soil erosion and increased nutrient loss in a small catchment. Sci. Total Environ. 648, 1097–1104.
Da Cunha, E R, Bacani, V M, Panachuki, E, 2017. Modeling soil erosion using RUSLE and GIS in a watershed occupied by rural settlement in the Brazilian Cerrado. Nat. Hazards 85 (2), 851–868.
Das, B, Paul, A, Bordoloi, R, Tripathi, O P, Pandey, P K, 2018. Soil erosion risk assessment of hilly terrain through integrated approach of RUSLE and geospatial technology: a case study of Tirap District, Arunachal Pradesh. Modeling Earth Systems and Environment 4 (1), 373–381.
Day, P R, 1965. Methods of soil analysis, Part I. Agronomy 9, 545–567.
Demirci, A, Karaburun, A, 2012. Estimation of soil erosion using RUSLE in a GIS framework: a case study in the Buyukcekmece Lake watershed, northwest Turkey. Environmental Earth Sciences 66 (3), 903–913.
Djoukbala, O, Mazour, M, Hasbaia, M, Benselama, O, 2018. Estimating of water erosion in semiarid regions using RUSLE equation under GIS environment. Environmental Earth Sciences 77 (9), 345.
Dutta, D, Das, S, Kundu, A, Taj, A, 2015. Soil erosion risk assessment in Sanjal watershed, Jharkhand (India) using geo-informatics, RUSLE Model and TRMM data. Modeling Earth Systems and Environment 1, 37. doi:10.1007/s40808-015-0034-1.
Ekholm, P, Lehtoranta, J, 2012. Does control of soil erosion inhibit aquatic eutrophication? J. Environ. Manag. 93 (1), 140–146.
Fang, G, Yuan, T, Zhang, Y, Wen, X, Lin, R, 2019. Integrated study on soil erosion using RUSLE and GIS in Yangtze river basin of jiangsu province (China). Arabian Journal of Geosciences 12 (5), 173.
Farhan, Y, Nawaiseh, S, 2015. Spatial assessment of soil erosion risk using RUSLE and GIS techniques. Environmental Earth Sciences 74 (6), 4649–4669.
Farhan, Y, Zregat, D, Farhan, I, 2013. Spatial estimation of soil erosion risk using RUSLE approach, RS, and GIS techniques: a case study of Kufranja watershed, Northern Jordan. J. Water Resour. Protect. 5 (12), 1247.
Fayas, C M, Abeysingha, N S, Nirmanee, K G S, Samaratunga, D, Mallawatantri, A, 2019. Soil loss estimation using rusle model to prioritize erosion control in KELANI river basin in Sri Lanka. International Soil and Water Conservation Research 7 (2), 130–137.
Ferreira, V, Panagopoulos, T, 2014. Seasonality of soil erosion under Mediterranean conditions at the Alqueva dam watershed. Environ. Manag. 54 (1), 67–83.
Fu, B J, Zhao, W W, Chen, L D, Zhang, Q J, Lü, Y H, Gulinck, H, Poesen, J, 2005. Assessment of soil erosion at large watershed scale using RUSLE and GIS: a case study in the Loess Plateau of China. Land Degrad. Dev. 16 (1), 73–85.
Fu, B, Liu, Y, Lü, Y, He, C, Zeng, Y, Wu, B, 2011. Assessing the soil erosion control service of ecosystems change in the Loess Plateau of China. Ecol. Complex. 8 (4), 284–293.
Ganasri, B P, Ramesh, H, 2016. Assessment of soil erosion by RUSLE model using remote sensing and GIS-A case study of Nethravathi Basin. Geoscience Frontiers 7 (6), 953–961.
García-Ruiz, J M, Nadal-Romero, E, Lana-Renault, N, Beguería, S, 2013. Erosion in Mediterranean landscapes: changes and future challenges. Geomorphology 198, 20–36.
Hao, C H E N, Oguchi, T, Pan, W U, 2017. Assessment for soil loss by using a scheme of alterative sub-models based on the RUSLE in a Karst Basin of Southwest China. Journal of integrative agriculture 16 (2), 377–388.
Haregeweyn, N, Tsunekawa, A, Nyssen, J, Poesen, J, Tsubo, M, TsegayeMeshesha, D, Tegegne, F, 2015. Soil erosion and conservation in Ethiopia: a review. Prog. Phys. Geogr. 39 (6), 750–774.
Hasan, I, Hammad, M, Ismail, K, 2014. Estimating the ratio between the amount of sediments related to water erosion of the soil and the amount of sediments transported in Zgaro River. Tishreen University Journal for Research and Scientific Studies - Engineering Sciences Series 36, 277–299 (in Arabic).
Inbar, M, Zgaier, A, 2016. Physical and social aspects of land degradation in mediterranean highland terraces: a geodiversity approach. Ann.: Anali istrske mediteranske studije. Ser. Hist. Sociol. 26 (3), 419–432.
Karydas, C G, Panagos, P, 2018. The G2 erosion model: an algorithm for month-time step assessments. Environ. Res. 161, 256–267.
Karydas, C G, Panagos, P, Gitas, I Z, 2014. A classification of water erosion models according to their geospatial characteristics. International Journal of Digital Earth 7 (3), 229–250.
Kayet, N, Pathak, K, Chakrabarty, A, Sahoo, S, 2018. Evaluation of soil loss estimation using the RUSLE model and SCS-CN method in hillslope mining areas. International Soil and Water Conservation Research 6 (1), 31–42.
Kbibo, I, Ibrahim, J, Bou-Issa, A, 2017. Studying the effect of soil erosion for eight different systems with different slopes in the coastal area under forests, burned forest and planted soil system. Tishreen University Journal for Research and Scientific Studies - Biological Sciences Series 39, 25–38 (In Arabic).
Kertész, Á, 2009. The global problem of land degradation and desertification. Hungarian Geographical Bulletin 58 (1), 19–31.
Lal, R, 1998. Soil erosion impact on agronomic productivity and environment quality. Crit. Rev. Plant Sci. 17 (4), 319–464.
Lu, D, Li, G, Valladares, G S, Batistella, M, 2004. Mapping soil erosion risk in Rondonia, Brazilian Amazonia: using RUSLE, remote sensing and GIS. Land Degrad. Dev. 15 (5), 499–512.
Mahala, A, 2018. Soil erosion estimation using RUSLE and GIS techniques—a study of a plateau fringe region of tropical environment. Arabian Journal of Geosciences 11 (13), 335.
Markose, V J, Jayappa, K S, 2016. Soil loss estimation and prioritization of sub-watersheds of Kali River basin, Karnataka, India, using RUSLE and GIS. Environ. Monit. Assess. 188 (4), 225.

Martínez-Casasnovas, J A, Sánchez-Bosch, I, 2000. Impact assessment of changes in land use/conservation practices on soil erosion in the Penedès–Anoia vineyard region (NE Spain). Soil Tillage Res. 57 (1–2), 101–106.

Masri, Z, Zöbisch, M, Bruggeman, A, Hayek, P, Kardous, M, 2003. Wind erosion in a marginal Mediterranean dryland area: a case study from the Khanasser Valley, Syria. Earth Surf. Process. Landforms: The Journal of the British Geomorphological Research Group 28 (11), 1211–1222.

Mohammed, S, Kbibo, I, Alshihabi, O, Mahfoud, E, 2016. Studying rainfall changes and water erosion of soil by using the WEPP model in Lattakia, Syria. J. Agric. Sci. 61 (4), 375–386.

Mohammed, S A, Alkerdi, A, Nagy, J, Harsányi, E, 2019. Syrian crisis repercussions on the agricultural sector: case study of wheat, cotton and olives. Regional Science Policy & Practice.

Mohammed, S, Khallouf, A, Alshiehabi, O, Pham, Q B, Linh, N T T, Anh, D T, Harsányi, E, 2020. Predicting soil erosion hazard in Lattakia governorate (W Syria). Int. J. Sediment Res..

Mohammed, S, Habi, H, Ali, H, Alhenawi, S, Kiwan, S, Ghanem, S, Harsányi, E, 2020. Soils of the Southern Syria-A big database for the future land management planning. Data in Brief 105832.

Moore, I D, Burch, G J, 1986. Physical basis of the length slope factor in the universal soil loss equation. Soil Sci. Soc. Am. J. 50 (5), 1294–1298.

Morgan, R C P, 1995. Soil Erosion and Conservation. Longman Group UK Limited, London, p. 198 p..

Morgan, R P C, 2005. Soil Erosion and Conservation. Third Ed Blackwell Science Ltd., p. 304, 1-4051-1781-8.

Nampak, H, Pradhan, B, MojaddadiRizeei, H, Park, H J, 2018. Assessment of land cover and land use change impact on soil loss in a tropical catchment by using multitemporal SPOT-5 satellite images and revised universal soil loss equation model. Land Degrad. Dev. 29 (10), 3440–3455.

Nasir, N, Selvakumar, R, 2018. Influence of land use changes on spatial erosion pattern, a time series analysis using RUSLE and GIS: the cases of Ambuliyar sub-basin, India. Acta Geophys. 66 (5), 1121–1130.

National Weather Service, 2000. Federal meteorological handbook no.1: surface weather observations and reports. In: Whiteman, C D (Ed.), Mountain Meteorology. Fundamentals and Applications. Oxford University Press, Oxford, p. 355 p.

Nearing, M A, Foster, G R, Lane, L J, Finkner, S C, 1989. A process-based soil erosion model for USDA-water erosion prediction project technology. Transactions of the ASAE 32, 1587–1593. doi:10.13031/2013.31195.

Nelson, D W, Sommers, L E, 1982. Methods of Soil Analysis. Part II (2nd Edition). Madismson, p. 1159.

Ollobarren Del Barrio, P, Campo-Bescós, M A, Giménez, R, Casalí, J, 2018. Assessment of soil factors controlling ephemeral gully erosion on agricultural fields. Earth Surf. Process. Landforms.

Ostovari, Y, Ghorbani-Dashtaki, S, Bahrami, H A, Naderi, M, Dematte, J A M, 2017. Soil loss prediction by an integrated system using RUSLE, GIS and remote sensing in semi-arid region. Geoderma Regional 11, 28–36.

Ozsoy, G, Aksoy, E, Dirim, M S, Tumsavas, Z, 2012. Determination of soil erosion risk in the Mustafakemalpasa River Basin, Turkey, using the revised universal soil loss equation, geographic information system, and remote sensing. Environ. Manag. 50 (4), 679–694.

Pal, S, 2016. Identification of soil erosion vulnerable areas in Chandrabhaga river basin: a multi-criteria decision approach. Modeling Earth Systems and Environment 2 (1), 5.

Pal, S, Debanshi, S, 2018. Influences of soil erosion susceptibility toward overloading vulnerability of the gully head bundhs in Mayurakshi River basin of eastern Chottanagpur Plateau. Environment. Development and Sustainability 20 (4), 1739–1775.

Panagos, P, Borrelli, P, Meusburger, K, Zanden, A H, Poesen, J, Alewell, C, 2015. Modelling the effect of support practices (P-factor) on the reduction of soil erosion by water at European scale. Environ. Sci. Pol. 51, 23–34. doi:10.1016/j.envsci.2015.03.012.

Paroissien, J B, Darboux, F, Couturier, A, Devillers, B, Mouillot, F, Raclot, D, Le Bissonnais, Y, 2015. A method for modeling the effects of climate and land use changes on erosion and sustainability of soil in a Mediterranean watershed (Languedoc, France). J. Environ. Manag. 150, 57–68.

Phinzi, K, Abriha, D, Bertalan, L, Holb, I, Szabó, S, 2020. Machine learning for gully feature extraction based on a pan-sharpened multispectral image: multiclass vs. Binary approach. ISPRS Int. J. Geo-Inf. 9 (4), 252.

Pieri, L, Poggio, M, Vignudelli, M, Bittelli, M, 2014. Evaluation of the WEPP model and digital elevation grid size, for simulation of streamflow and sediment yield in a heterogeneous catchment. Earth Surf. Process. Landforms 39 (10), 1331–1344.

Pimentel, D, Burgess, M, 2013. Soil erosion threatens food production. Agriculture 3 (3), 443–463.

Prasannakumar, R, Shiny, N, Geetha, H, Vijith, H, 2011. Spatial prediction of soil erosion risk by remote sensing, GIS and RUSLE approach: a case study of Siruvani river watershed in Attapady valley, Kerala, India. Environ Earth Sci 64, 965–972.

Prasannakumar, V, Vijith, H, Geetha, N, Shiny, R, 2011. Regional scale erosion assessment of a sub-tropical highland segment in the Western Ghats of Kerala, South India. Water Resour. Manag. 25 (14), 3715.

Prasannakumar, V, Vijith, H, Abinod, S, Geeth, N, 2012. Estimation of soil erosion risk within a small mountainous sub-watershed in Kerala, India, using Revised Universal Soil Loss Equation (RUSLE) and geo-information technology. Geoscience Frontiers 3 (2), 209–215.

Raclot, D, Le Bissonnais, Y, Louchart, X, Andrieux, P, Moussa, R, Voltz, M, 2009. Soil tillage and scale effects on erosion from fields to catchment in a Mediterranean vineyard area. Agric. Ecosyst. Environ. 134 (3–4), 201–210.

Remke, A, Rodrigo-Comino, J, Gyasi-Agyei, Y, Cerdà, A, Ries, J B, 2018. Combining the stock unearthing method and structure-from-motion photogrammetry for a gapless estimation of soil mobilisation in vineyards. ISPRS Int. J. Geo-Inf. 7 (12), 461.

Renard, K G, Foster, G R, Weesies, G A, Porter, J P, 1991. RUSLE: revised universal soil loss equation. J. Soil Water Conserv. 46, 30–33.

Renard, K G, Foster, G R, Weesies, G A, McCool, D K, Yoder, D C, 1997. "Predicting Soil Erosion by Water: A Guide to Conservation Planning with the Revised Universal Soil Loss Equation (RUSLE)." Agriculture Handbook No. 703. U.S. Dept. of Agriculture, Washington, DC.

Rodrigo-Comino, J, 2018. Five decades of soil erosion research in "terroir". The State-of-the-Art. Earth Sci. Rev. 179, 436–447.

Rodrigo-Comino, J, Keesstra, S, Cerdà, A, 2018. Soil erosion as an environmental concern in vineyards: the case study of Celler del Roure, Eastern Spain, by means of rainfall simulation experiments. Beverages 4 (2), 31.

Rodrigo-Comino, J, Giménez-Morera, A, Panagos, P, Pourghasemi, H R, Pulido, M, Cerdà, A, 2019. The potential of straw mulch as a nature-based solution in olive groves treated with glyphosate. A biophysical and socio-economic assessment. Land Degrad. Dev. 1–13.

Sarapatka, B, Cap, L, Bila, P, 2018. The varying effect of water erosion on chemical and biochemical soil properties in different parts of Chernozem slopes. Geoderma 314, 20–26.

Sujatha, E, Sridhar, V, 2018. Spatial prediction of erosion risk of a small mountainous watershed using RUSLE: a case-study of the palar sub-watershed in kodaikanal, south India. Water 10 (11), 1608.

Taye, G, Vanmaercke, M, Poesen, J, Van Wesemael, B, Tesfaye, S, Teka, D, Haregeweyn, N, 2018. Determining RUSLE P-and C-factors for stone bunds and trenches in rangeland and cropland, North Ethiopia. Land Degrad. Dev. 29 (3), 812–824.

Thomas, J, Joseph, S, Thrivikramji, K P, 2018. Assessment of soil erosion in a tropical mountain river basin of the southern Western Ghats, India using RUSLE and GIS. Geoscience Frontiers 9 (3), 893–906.

Toubal, A K, Achite, M, Ouillon, S, Dehni, A, 2018. Soil erodibility mapping using the RUSLE model to prioritize erosion control in the Wadi Sahouat basin, North-West of Algeria. Environ. Monit. Assess. 190 (4), 210.

Tuo, D, Xu, M, Gao, G, 2018. Relative contributions of wind and water erosion to total soil loss and its effect on soil properties in sloping croplands of the Chinese Loess Plateau. Sci. Total Environ. 633, 1032–1040.

Wessels, K J, Prince, S D, Malherbe, J, Small, J, Frost, P E, VanZyl, D, 2007. Can human-induced land degradation be distinguished from the effects of rainfall variability? A case study in South Africa. J. Arid Environ. 68 (2), 271–297.

Wischmeier, W H, Smith, D D, 1965. Predicting Rainfall-Erosion Losses from Cropland East of the Rocky Mountains: Guide for Selection of Practices for Soil and Water Conservation. USDA Agricultural Handbook p. 282.

Wischmeier, W H, Smith, D D, 1978. Predicting Soil Erosion Losses: A Guide to Conservation Planning. USDA Agricultural Handbook p. 537.

Woldemariam, G W, Iguala, A D, Tekalign, S, Reddy, R U, 2018. Spatial modeling of soil erosion risk and its implication for conservation planning: the case of the gobele watershed, east hararghe zone, Ethiopia. Land 7 (1), 25.

Zerihun, M, Mohammedyasin, M S, Sewnet, D, Adem, A A, Lakew, M, 2018. Assessment of soil erosion using RUSLE, GIS and remote sensing in NW Ethiopia. Geoderma regional 12, 83–90.

Zhao, J, Yang, Z, Govers, G, 2019. Soil and water conservation measures reduce soil and water losses in China but not down to background levels: evidence from erosion plot data. Geoderma 337, 729–741.

Zhu, M, 2012. Soil erosion risk assessment with CORINE model: case study in the Danjiangkou Reservoir region, China. Stoch. Environ. Res. Risk Assess. 26 (6), 813–822.